

# Simulation of crack opening through a corner node, using rigid-plastic interface elements

D. Ciancio & I. Carol

*ETSECCPB, Technical University of Catalonia UPC, Barcelona, Spain*

M. Cuomo

*Dept. of Civil and Environmental Engineering, University of Catania, Catania, Italy*

**ABSTRACT:** Recently, the authors of this paper have proposed a new technique based on a double minimization with respect to a Mohr circle, for the computation of stresses and forces transmitted across mesh lines at the corner nodes of FE mesh in 2D (Ciancio et al. 2006). That procedure establishes the basis for the general modeling of crack development along mesh lines without the need of the onerous systematic pre-insertion of zero thickness interface elements with elastic compliance and duplicated nodes from the beginning of the analysis. In this context, the present paper goes one step further, focusing on the crack opening conditions for a set of mesh lines (also interpreted as rigid plastic interfaces) which concur on an inner node of the FE mesh. The cracking condition is assumed in the form of rigid plasticity in terms of the stress traction components. With those assumptions, the state of cracking at the node undergoes in general three different stages of evolution. For each of them, the appropriate procedure for the calculation of the corresponding forces and stresses is presented, and the overall scheme is illustrated with some examples of application.

## 1 INTRODUCTION

Zero thickness interface elements have been used quite successfully since the late 80s to simulate fracture problems in concrete and other quasi-brittle materials (Rots 1988, Rots et al. 1990, Sluys & Berends 1998, Carol et al. 2001, Caballero et al. 2006.). These interface elements, which are inserted along the mesh lines, exhibit double nodes and are in general equipped with elasto-plastic or damage constitutive laws involving penalty-type elastic stiffness  $K$  of very high but finite value. Among the advantages of these elements is the natural easy way in which they can be incorporated in standard FE codes and strategies.

However, on the negative side are: 1) extremely high values of  $K$  used to minimize spurious interface compliance can generate ill-conditioning problems, and 2) the duplication of nodes due to the insertion of interfaces may increase dramatically the computational effort for the solution of the overall problem. In attempting to overcome these difficulties, some procedures have been proposed to detect crack opening conditions along mesh lines of a standard FE mesh, and to insert interfaces only along those lines effectively cracked (Camacho & Ortiz 1996). However, in the literature, those procedures were limited to middle nodes of quadratic elements, only location

at which the evaluation of inter-element forces becomes trivial.

In this context, the authors of this paper have recently proposed a new procedure for the evaluation of inter-element forces transmitted across the mesh lines concurring at a “corner” node of a standard FE mesh. The procedure (Ciancio et al. 2006) is based on a double minimization of the (unknown) stress tractions across such mesh lines with respect to the projections of the (also unknown) stress tensor at the same node. It can be applied to linear or quadratic elements and it leads to very satisfactory results in all examples analyzed, with the added bonus of providing also the nodal stresses and therefore fulfilling the role of a cheap, effective and advantageous stress “smoothing” technique. In the present paper, the authors take one step further and use that procedure to evaluate crack opening conditions at the corner nodes of the mesh. The study is developed without *a priori* systematic insertion of elastic interface elements, and assuming each line of the mesh as a potential crack, the opening of which is governed by a rigid-plastic model. Due to this, and to the fact that in the case of crack opening an interface element would indeed have to be inserted along that line, one can understand the procedure as dealing with rigid-plastic interface element which stay totally closed until cracking conditions are exceeded.

## 2 BASIC CONCEPTS AND ASSUMPTIONS

The present study assumes that continuum elements behave linearly elastic and all the potential cracks are initially closed. External load is characterized by an increasing load factor  $\mu$ . Because the study focuses on the phenomena happening until the opening of the first crack at a node, the overall FE calculation may be considered as linear elastic during the entire study.

### 2.1 Possible crack mechanisms

The most general mechanisms of growth and propagation of a crack through the interior corner node of a common FE mesh are illustrated in Figure 1. In any circumstance, the formation of a crack implies the separation of lines and the duplication (or triplification) of nodes. When a crack nucleates or propagates through a corner node, at least two mesh lines separate. It means that the failure conditions must be simultaneously satisfied at least by two interfaces. This simple statement is crucial for the understanding of the kinematic conditions for the formation of a crack.

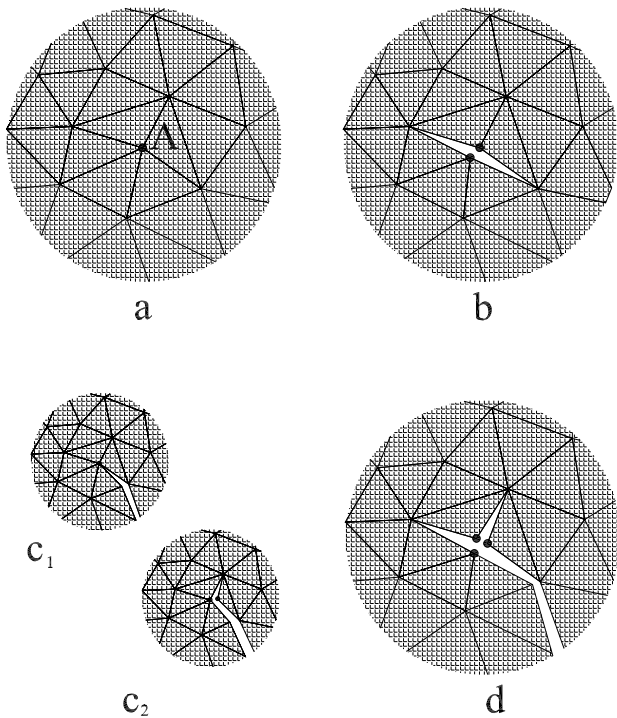


Figure 1. In a) interior corner node A of a generic FE mesh; in b) nucleation of a crack through node A; in c) propagation of a crack through node A; in d) bifurcation of a crack through A.

### 2.2 Interface rigid plastic constitutive law

As previously mentioned, each mesh line acts as a potential predefined path for the formation of a crack. Thus, each mesh line can be considered as a rigid-plastic interface element that remains closed provided that some failure opening conditions are not satisfied. The failure surface is defined in the standard way by means of a scalar function  $F$  equal

to  $F(\mathbf{t}, \mathbf{p})$ , where  $\mathbf{t}$  denotes the stress vector in terms of normal and shear components  $(\sigma, \tau)$ , and  $\mathbf{p}$  denotes a collection of parameters which define the shape and the size of the surface and that in general evolve during the crack process.

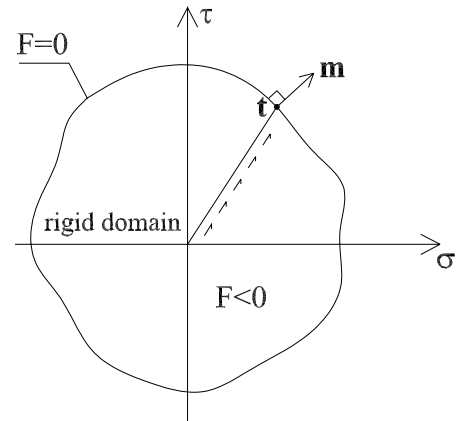


Figure 2. Failure surface  $F$  defined in the normal  $\sigma$  and tangential  $\tau$  stress plane. The vector  $\mathbf{m}$  is the flow rule vector associated to the tractions  $\mathbf{t}$  and assigning the direction of the irreversible relative opening displacement vector  $\mathbf{w}$ .

According to plasticity, as stress tractions increase at the interface, two situations may occur:

- $F(\mathbf{t}, \mathbf{p}) < 0$ , i.e. stress tractions are still inside the rigid domain, thus the interface remains closed;
- $F(\mathbf{t}, \mathbf{p}) = 0$ , i.e. stress tractions have reached the fracture surface (see Fig. 2).

Note that, as in plasticity,  $F > 0$  is not allowed, and that the cracking criterion  $F(\mathbf{t}, \mathbf{p}) = 0$  is only a necessary condition for crack opening. In the case that the crack would start to open, the opening direction will be given by a flow rule vector  $\mathbf{m}$  in a way also similar to standard plasticity, that is:

$$\dot{\mathbf{w}} = \lambda \mathbf{m} = \lambda \begin{pmatrix} \frac{\partial P}{\partial \sigma} \\ \frac{\partial P}{\partial \tau} \end{pmatrix} \quad (1)$$

in which  $\mathbf{w}$  is the relative opening displacement of the crack,  $\lambda$  is a scalar multiplier indicating the intensity of the opening, and  $\mathbf{m}$  is the direction of the displacement or flow rule (see Fig. 2). This direction may be conveniently defined as the gradient of  $P$ , being  $P$  the plastic potential, which is equal to  $F$  if the model is associated. The rest of the rigid-plastic crack opening model is not defined since not strictly required for the purpose of this study.

## 3 THE THREE STAGES BEFORE THE OPENING OF A CRACK

The values of stress tractions across the mesh lines concurrent at an interior corner node of the mesh must be calculated first, in order to determine the opening conditions of a crack through that same node. Simple equilibrium equations are not suffi-

cient to obtain these variables. A procedure is needed as a post-process of the standard FE calculation. For a purely rigid state (before any other crack has opened), this procedure has been recently developed by the authors of this paper (Ciancio et al. 2006) and it is briefly presented in the following.

On the left side of Figure 3 an interior node of a generic FE mesh is represented, to which  $N$  elements are connected. On the right side, the nodal forces  $\mathbf{f}_i$  ( $i=1,N$ ) obtained by a standard FE calculation and the nodal inter-element forces  $\mathbf{r}_i$  (that represent the unknowns of the problem) are reported.

Establishing elementary equilibrium equations at each element tip between equilibrium nodal forces and the two inter-element forces on each side, and making a simple trivial count, one obtains that there are  $2N$  unknown variables while only  $2N-2$  linear independent equilibrium equations. Thus, the inter-element forces are undetermined and their values depend on two arbitrary parameters, which for the sake of convenience are chosen equal to the components of one the inter-element force vectors denoted as  $\bar{\mathbf{r}}$ . Now, a procedure is established to determine these two arbitrary variables. For each interface, the nodal inter-element force, initially unknown, is directly related to the inter-element stresses or stress tractions  $\mathbf{t}$  via the contributing area concept:

$$\mathbf{t}_i = \begin{pmatrix} \sigma_i \\ \tau_i \end{pmatrix} = \frac{1}{\Omega_i} \mathbf{Q}_i \begin{pmatrix} r_{xi} \\ r_{yi} \end{pmatrix} \quad (2)$$

where  $\Omega_i$  stands for the contributing area (this area can be determined using the principle of virtual work in a way similar to the standard procedure to calculate nodal forces equivalent to external distributed forces), and  $\mathbf{Q}_i$  stands for the rotation matrix from the global ( $\mathbf{x}, \mathbf{y}$ ) to the local ( $\mathbf{n}_i, \mathbf{s}_i$ ) reference system (see Fig. 3).

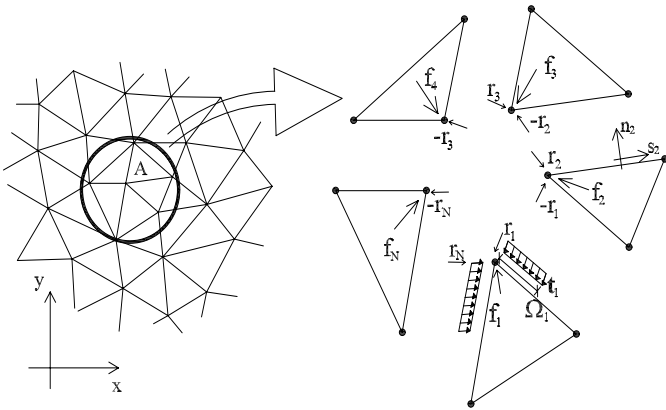


Figure 3. On the left, an interior corner node of a generic FE mesh is illustrated. On the right, the  $N$  element  $\mathbf{f}$  and inter-element  $\mathbf{r}$  nodal forces are enlightened, as well as the constant distribution of the inter-element stresses along the contributive area  $\Omega$  and the local reference system ( $\mathbf{n}, \mathbf{s}$ ).

At the same point (corner node), an *a priori* unknown nodal stress tensor  $\mathbf{T}$  is defined, and the following minimization function is considered:

$$\Phi = \sum_{i=1}^N \left( (\sigma_i - \mathbf{n}_i \cdot \mathbf{T} \cdot \mathbf{n}_i)^2 + (\tau_i - \mathbf{s}_i \cdot \mathbf{T} \cdot \mathbf{n}_i)^2 \right) \quad (3)$$

in which the differences between the equilibrated stress tractions (obtained by Equation 2) and the projections of the (unknown) nodal stress tensor, along the normal and tangential directions, are squared and summed for all the mesh lines converging onto the corner node. Note that, by virtue of the nodal equilibrium equations, the inter-element equilibrated stress tractions may be ultimately expressed in terms of the two scalar variables contained in the arbitrary indeterminate vector  $\bar{\mathbf{r}}$ . Therefore, the scalar function in Equation 3 depends on the three components of  $\mathbf{T}$  and on the two components of  $\bar{\mathbf{r}}$ .

The missing equations are obtained by the double minimization of Equation 3. First, it is assumed that the arbitrary force  $\bar{\mathbf{r}}$  is known, and the values of the components of the nodal stress tensor  $\mathbf{T}$  that minimize  $\Phi$  are obtained by setting equal to zero the derivatives of  $\Phi$  with respect to those same three components. This has to be done in closed form, since the arbitrary force is actually not known in advance, and the resulting expressions are functions of those two arbitrary force components. Then, from the three new equations obtained, the components of the nodal stress tensor are isolated and substituted back into the expression of Equation 3, so that the minimization function becomes actually a function of the two components of  $\bar{\mathbf{r}}$  only. Then a second minimization of the function is performed, also in closed form, this time with respect to the two components of the arbitrary inter-element force  $\bar{\mathbf{r}}$ .

The result of the above derivation turns out surprisingly simple, leading to the linear system:

$$\mathbf{D} \cdot \bar{\mathbf{r}} - \mathbf{d} = \mathbf{0} \quad (4)$$

from which the values of the  $\bar{\mathbf{r}}$  components can be easily obtained as the solution of a  $2 \times 2$  linear system. From these, using previous equations one can recover all the inter-element forces and stresses, as well as the nodal stress tensor. The values obtained in this way have been verified in several examples, and they turn out to be always exact for a uniform stress state (i.e. the nodal stress tensor  $\mathbf{T}$  coincides with the prescribed stress state on the overall mesh, and all the stress tractions  $\mathbf{t}$  sit on the corresponding Mohr circle). For a non-uniform stress state, the stress tractions may not sit exactly on the circle, and the circle itself may not coincide exactly with the expected stress state. However, they represent the best fit possible by the least square criteria employed, depending on the degree of refinement of the mesh and on the approximation order of the finite elements used (linear, quadratic, etc). In any case, the overall accuracy always turns out to be (at least) equal or (generally) better than the results obtained with alternative available techniques such as the stress average smoothing procedure. In the reference

paper (Ciancio et al. 2006), the above theory is also extended to corner nodes on the domain boundary, as well as on the interface between two materials.

### 3.1 Stage 1: cracking criterion reached by one single line

The previous derivation to obtain inter-element tractions is only valid while all of the resulting stress tractions on the mesh lines converging onto the corner node remain inside the cracking criterion in Mohr space, as for instance depicted on the left part of Figure 4. But for increasing external loads, eventually, one of the lines will reach the failure criterion. For the first line crack at the first node in the FE mesh, this *contact point* may be easily located by numerical (e.g. mid-point algorithm) or analytical procedures (e.g. see closed-form solutions for contact points in hyperbolic loading surfaces in Gens et al. 1988), leading to the specific value of the external loading factor  $\mu_1$ , for which this condition takes place. From this point on, for an increasing external loading factor, the formulation must change since otherwise the cracking criterion would be exceeded at that crack line, something it was assumed not possible in the previous section.

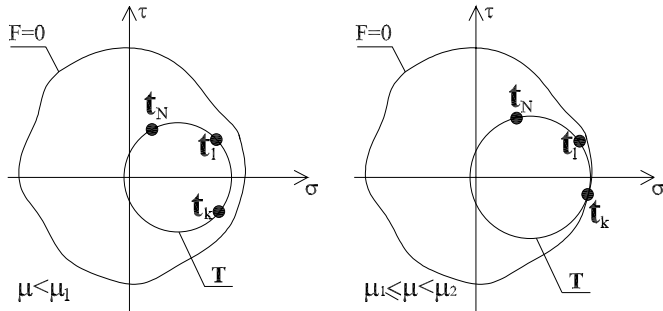


Figure 4. On the left: “stage 0”, i.e. the tractions are inside the rigid domain. On the right: “stage 1”, i.e. the nodal stresses of one interface  $\mathbf{t}_k$  has reached the fracture surface  $F(\mathbf{t}_k)=0$ .

On the other hand, the question may arise whether at this point a crack may already open through the corner node. This is, however, not possible since kinematic compatibility at the node implies that, if two element tips detached from each other, two (and not only one) lines at least would have to exhibit crack opening and therefore also would have to have reached the cracking criterion, which at this “stage 1” is not the case yet. The situation is represented in the right side of Figure 4, where the stress traction on one of the lines ( $\mathbf{t}_k$  in the example) is already on the cracking surface while the others are not.

For increasing external loading factor beyond the first contact point ( $\mu > \mu_1$ ), the stress tensor at the

node and the corresponding line tractions must still grow, except for the mesh line for which the cracking criterion has been reached, for which stress tractions are subjected to the condition  $F(\mathbf{t}_k)=0$ , which means that they can remain constant or “slide” on the cracking surface.

In this way, the previous condition acts as a constraint on the double minimization formulation previously developed for “stage 0”.

One way to introduce this constraint into the formulation without the need of Lagrange multipliers consists of:

- 1 choosing the arbitrary inter-element force as that corresponding to the line for which the cracking criterion has been reached, i.e.  $\bar{\mathbf{r}} = \Omega_k \mathbf{Q}_k \mathbf{t}_k$  (inverse of Equation 2);
- 2 using a specific cracking criterion expression to relate the two components of the stress traction on that line, and therefore reducing the arbitrary variables from two (the components of  $\bar{\mathbf{r}}$  in the global reference system  $\mathbf{x}, \mathbf{y}$ ) to one (one component of the stress traction).

From the expression  $F(\sigma_k, \tau_k)=0$  one can obtain the normal component  $\sigma$  as a function of  $\tau$ . Thus doing, the tractions laying on the fracture surface  $F$  may be expressed in vector form as:

$$\mathbf{t}_k = \begin{pmatrix} \sigma_k \\ \tau_k \end{pmatrix} = \begin{pmatrix} \sigma(\bar{\tau}) \\ \bar{\tau} \end{pmatrix} \quad (5)$$

which means that the only arbitrary variable in the system is now the shear component  $\tau_k$  at the line having reached the cracking criterion, which for convenience has been renamed as  $\bar{\tau}$ .

By using previous relation in Equation 5, the original arbitrary forces  $\bar{\mathbf{r}}$  may also be expressed in terms of the only unknown  $\bar{\tau}$ :

$$\bar{\mathbf{r}} = \Omega_k \mathbf{Q}_k \mathbf{t}_k = \bar{\Omega} \bar{\mathbf{Q}} \begin{pmatrix} \sigma(\bar{\tau}) \\ \bar{\tau} \end{pmatrix} \quad (6)$$

and therefore all the remaining  $N-1$  inter-element forces and stresses may also be expressed in terms of the same single arbitrary variable  $\bar{\tau}$ . Under these conditions, the same objective function  $\Phi$  as in previous subsection is considered, although now it only needs to be minimized with respect to  $\bar{\tau}$ . This is done by using the chain rule:

$$\frac{\partial \Phi}{\partial \bar{\tau}} = \frac{\partial \Phi}{\partial \bar{\mathbf{r}}} \frac{\partial \bar{\mathbf{r}}}{\partial \bar{\tau}} = 0 \quad (7)$$

The last term of previous equation, renamed for simplicity  $\bar{\mathbf{r}}$ , may be simply evaluated by differentiation of Equation 6.

Taking into account now that the derivative of  $\Phi$  with respect to  $\bar{\mathbf{r}}$  is the same as in Equation 4, previous Equation 7 can be finally written as:

$$\frac{\partial \Phi}{\partial \bar{\tau}} = \bar{\mathbf{r}}^{\prime T} \cdot \mathbf{D} \cdot \bar{\mathbf{r}} - \bar{\mathbf{r}}^{\prime T} \cdot \mathbf{d} = 0 \quad (8)$$

This actually constitutes a scalar equation from which the value of  $\bar{\tau}$  can be obtained. Once  $\bar{\tau}$  is known, the inter-element forces of all the mesh lines around the corner node can be computed using Equation 6 and the nodal equilibrium equations.

### 3.2 Stage 2: cracking criterion reached by two lines

The derivation presented for “stage 1” in previous section, is valid as long as only one line converging on that node has reached the cracking criterion while the others still have not. But of course, if the external loading factor  $\mu$  keeps increasing (and lets remember here that from the structural/FE viewpoint this is still a linear elastic calculation, since no cracks have opened yet), the cracking criterion will eventually be also satisfied for a second potential crack line. Similar to previous section, the new contact point may be located by numerical or analytical procedures, leading to the specific value of the external loading factor  $\mu_2$  for which this second contact takes place. From this point on, for an increasing external loading factor, the formulation must change, since otherwise the cracking criterion would be exceeded at that second crack line, something it was assumed not possible in the previous section.

On the other hand, the question may arise again whether at this point, with two lines converging on the same node having reached cracking criterion, a crack may already open through the corner node and be “visible” at the structural/FE level. However, in the general case these conditions are still not sufficient for crack opening, due to the flow rule assumptions defined together with the cracking criterion in Section 1. The flow rule defines the direction of the opening for each of the cracks independently and it must also be satisfied simultaneously by the two cracks. As illustrated in Figure 5, the coincidence of the flow rule for the two cracking lines in the global coordinate system is not automatically ensured only by the fact that the cracking criterion is met for both of them. In fact, calculations show that in general this is not the case, which means that, in spite of satisfying the failure conditions for both lines, the crack cannot open yet due to kinematic incompatibility.

This situation of two concurring crack lines in failure state but without being able to open, will be maintained until the flow rules get realigned, which in general will take place for a higher loading factor  $\mu_3 > \mu_2$ .

The formulation for evaluating inter-element forces and stresses during “stage 2” with  $\mu_2 < \mu < \mu_3$ , does not require any minimization. As already said in previous subsections, basic equilibrium at each

element tip between equilibrated nodal forces obtained from the FE analysis and inter-element forces provides  $2N-2$  equations. The cracking criterion applied to the two cracking lines provides two additional equations, totaling  $2N$ , which coincides with the number of the unknown components (two for each of the  $N$  inter-element forces or stresses).

One procedure to solve the system is to write the failure criterion  $F$  for each of the cracking lines denoted by indices  $k$  and  $i$ :

$$\begin{aligned} \tau_k &= \tau_k(\sigma_k) \\ \tau_i &= \tau_i(\sigma_i) \end{aligned} \quad (9)$$

Using Equation 2, the  $2N-2$  independent equations of equilibrium of the nodal forces can be rewritten in terms of  $N$  nodal inter-element stresses  $\mathbf{t}$ . Adding to this system the two failure criterion equations in Equation 9 for the cracking lines  $i$  and  $k$ , one gets a system whose number of unknown is equal to the number of equations, and that, for this reason, may be solved in closed form.

Note that the system coefficients involve the equilibrated FE forces on the concurrent element tips, and therefore the entire solution depends on the overall loading factor  $\mu$ . Furthermore, the system may or not be linear depending on the particular expression used for the failure function  $F$ .

### 3.3 Stage 3: onset of crack opening

The formulation developed for stage 2 will be valid only until the kinematic compatibility for crack opening is achieved. This may actually happen in two ways:

- 1 the stress tractions for one or more of the remaining mesh lines (other than the two already on the cracking surface) also reach the cracking condition  $F(\mathbf{t}_l) = 0$  with  $l \neq k, i$  or
- 2 the flow rules of the two cracking lines become parallel.

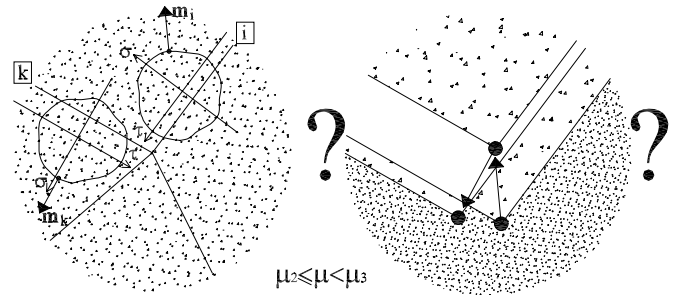


Figure 5. Kinematic incompatibility when the flow rule vectors of two different lines concurrent to a node ( $k$  and  $i$  in the figure) are not parallel.

In the first case, i.e. if one (or more) additional line(s) reaches the cracking criterion before the flow rules of the two original cracking lines of stage 2 become parallel, the onset of cracking is actually reached on the only condition that the various flow

rules constitute a set of linearly dependent vectors. This can be easily understood by considering that once cracks start opening, kinematic compatibility requires that the sum of the various relative displacements for each opening crack should be zero. Given the arbitrary value of the inelastic multipliers, the satisfaction of this condition is practically ensured with three or more opening cracks, except if some of the flow rules would happen to be parallel, which could cause the remaining one to be linearly independent from the rest. This could happen for instance in a triple crack if two of the cracking lines are on opposite sides of the node and have the same orientation (in which case in practice they could be considered as a single ‘through’ crack line). Except in these special situations, when a third line reaches cracking conditions the onset of cracking at the node is usually attained.

If the second condition above is satisfied first (i.e. the flow rules of the two cracking lines from stage 2 become parallel before any other line reaches the cracking criterion), that also marks the onset of cracking at the node. The opening crack is composed of two cracking lines that in general are not aligned and, therefore, the opening crack will exhibit a kink at the node, as shown in Figure 6.

The identification of the precise loading factor  $\mu_3$  for which this second condition takes place may be done in two ways:

(1) *via incremental computations*, i.e. by increasing the external loading factor by small steps, repeating each time the calculations of stage 2 and verifying the direction of the corresponding flow rules until they coincide, or

(2) *via limit analysis*, i.e. the loading factor  $\mu_3$  that satisfies the parallelism condition is considered as an unknown of the problem.

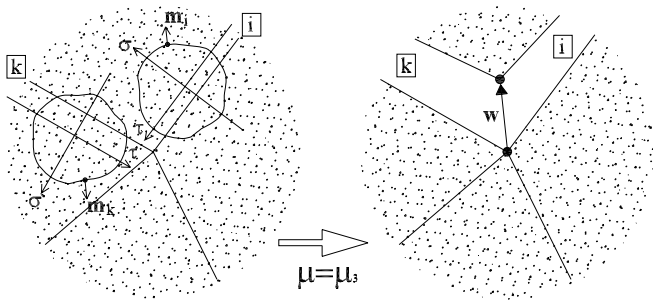


Figure 6. Parallel condition (on the left side) of the flow rule vectors  $\mathbf{m}_i$  and  $\mathbf{m}_k$  of two lines concurrent to a corner node allows crack opening (on the right side of the figure).

Further details on this method are given in Ciancio et al. (in press). Independently of what method is used, when the flow rule coincidence is detected, stage 3 is achieved and the real opening of the crack becomes possible at FE level, marking the end point of the current study.

Note that when two of the mesh lines have the same orientation and are located on opposite sides of the node, a straight crack becomes possible, and stage 2 and 3 may happen at the same time, i.e. when failure conditions are achieved for the second crack, at the same time flow rules turn out to be just parallel and the onset of crack opening is reached. In a similar way, under special conditions of geometrical and loading symmetry, it may happen that failure conditions are reached simultaneously for two crack lines, and so stage 1 and 2 would merge as well. But under general conditions, the three stages should exist, as it will be illustrated in the following application example.

#### 4 EXAMPLE

The example of application consists of the mesh and loads depicted in Figure 7. The ‘‘corner nodes’’ under study are the central node number 7 onto which four potential crack lines converge, and nodes number 4, 5, 9 and 10, onto which three potential cracking lines concur. The mesh is made up of linear triangles elements, which are assumed linear elastic. The mechanical parameters of the elastic continuum are:  $E=1000$  MPa and  $\nu=0.2$ . The specimen is 14 mm wide and 18 mm high. The boundary conditions are represented on the left side of Figure 7. The uniform stress state applied along the vertical direction is twice the stress along the horizontal direction. A loading factor  $\mu$  gives the increment of the applied load, whose nominal value is  $p_0=20$  MPa. The analysis is performed in plane stress.

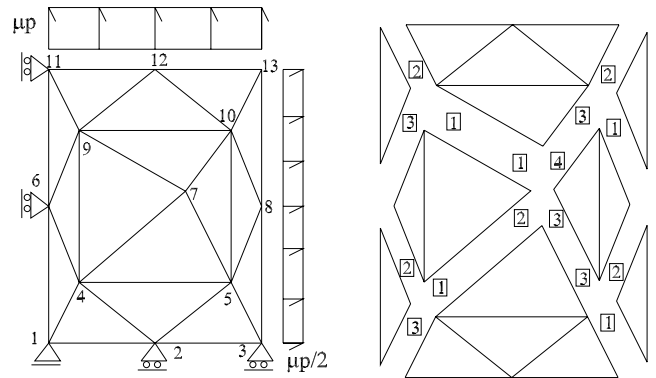


Figure 7. Mesh used as example in Section 4. On the left: boundary conditions; on the right, potential crack lines.

On the right side of Figure 7, the potential cracking lines of the mesh are explicitly represented. The cracking criterion for these lines is the hyperbolic failure surface presented by Carol et al. 1997, thus that  $F = \tau^2 - (c - \sigma \tan \phi)^2 + (c - \chi \tan \phi)^2$ . The parameters of the hyperbola are:  $\chi=20$  MPa,  $c=16.92$  MPa and  $\tan \phi=0.5$ . The other lines concurrent to

nodes 4, 5, 9 and 10 are not taken into consideration as cracking lines.

For the loading factor value of  $\mu=1.0$ , the cracking surface is reached on line 1 at node 7, as well as on line 1 at node 9. The tractions along the other lines in the mesh stay inside the cracking criterion. The results at this stage are shown in Figure 8 in which black dots represent the stress tractions  $\mathbf{t}$ , circles represent the stress states  $\mathbf{T}$  and hyperbolas represent the failure surface.

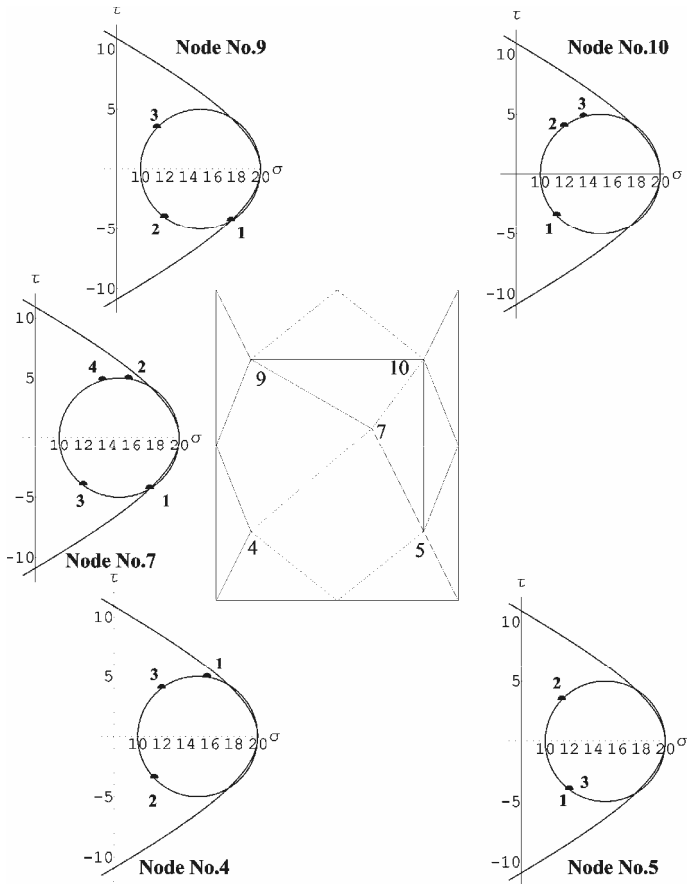


Figure 8. Stage 1 for node 7 and 9 (one of the potential cracking lines satisfies the cracking criterion); stage 0 for nodes 4, 5 and 10 (the stresses along the cracking lines are inside the rigid doain).

For  $\mu=1.058855857$  the situation at node 7 is the following: the traction vector for cracking line number 1 has been moving tangentially to the fracture surface until the tractions across cracking line number 4 have also satisfied the cracking criterion. This state represents the end of stage 2 for node 7 (as showed in Fig. 9) At node 9 the stresses of line number 1 remains on the cracking surface, but no other lines have reached the fracture surface for  $1 < \mu < 1.0588558$ . At node 4, for  $\mu=1.049557683$ , the stresses for line number 1 has attained the cracking criterion, and until  $\mu=1.058855857$  no other lines have reached this condition. At nodes 5 and 10 no lines have reached the cracking criterion.

For  $\mu=1.067790745$ , node 7 reaches the onset of cracking condition (stage 3) since the flow vectors of the cracking line 1 and 4 concurrent at this node

become parallel. Nodes 4 and 9 remain in stage 1, and nodes 5 and 10 in stage 0. All this is represented in Figure 10.

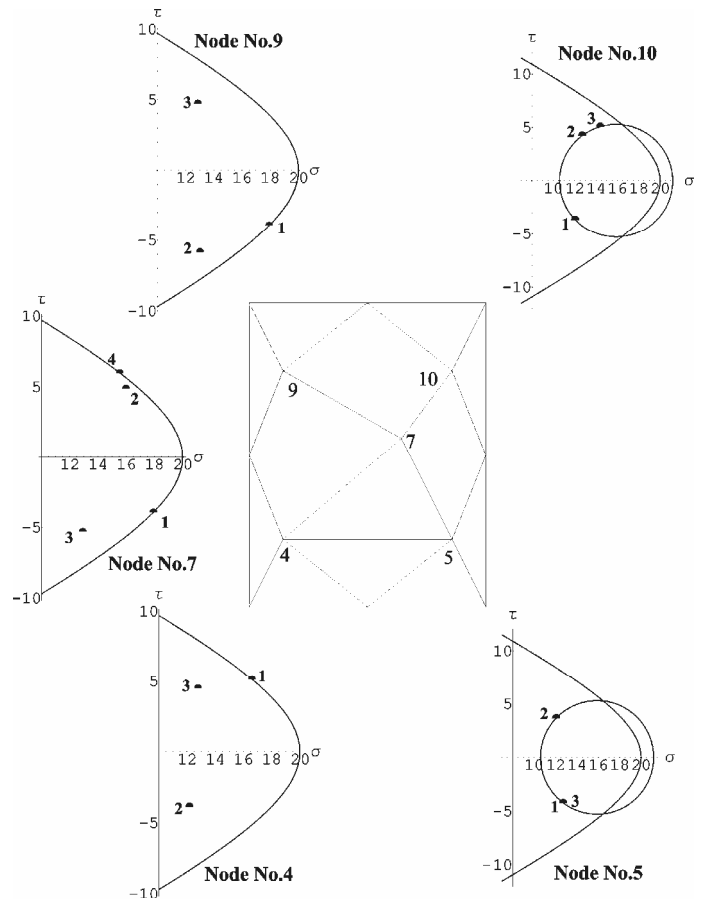


Figure 9. Stage 2 for node 7 (the tractions of two cracking lines lay on the fracture surface, but they still no satisfy the kinematic compatibility for the opening of a crack); stage 1 for nodes 4 and 9; stage 0 for nodes 5 and 10.

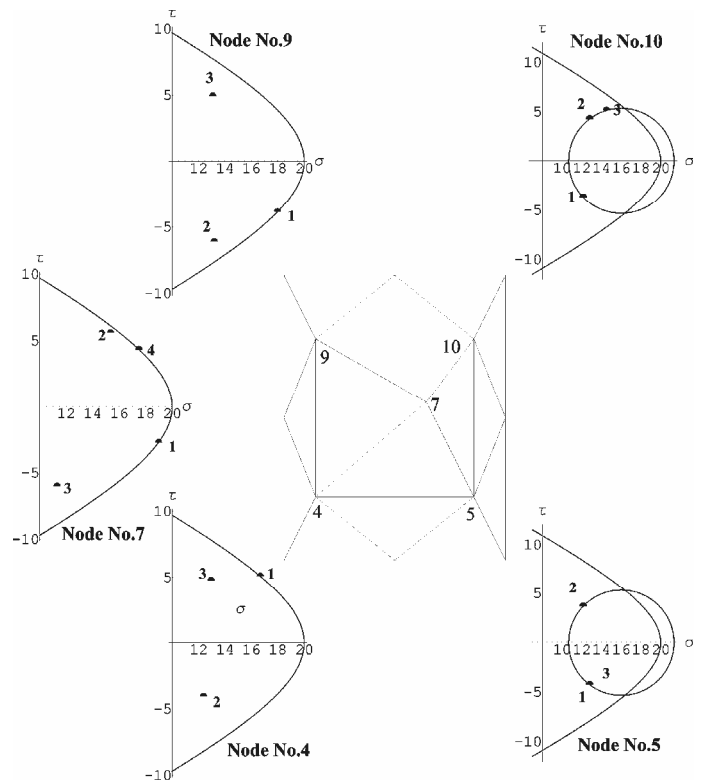


Figure 10. Stage 3 for node 7 (the flow rule vectors of the cracking line number 1 and 4 are parallel); stage 1 for nodes 4 and 9; stage 0 for nodes 5 and 10.

This point would indicate the beginning of the non-linear analysis with one opening crack through lines 1 and 4, and, therefore, it marks the end of the current study devoted to clarify the conditions and stages until crack opening may occur.

Note that, for the whole range between  $\mu=0$  and the onset of crack opening at  $\mu=1.067790745$ , the stress state at the Gauss points of the continuum triangular elements is uniform and equal to the external applied load ( $\sigma_x = \mu p/2$ ,  $\sigma_y = \mu p$ ). In contrast, during this loading process and after  $\mu=1.0$ , the stress tractions along mesh lines that are potential cracks, undergo some redistribution as the cracking criterion is progressively reached. This has been shown by the different values of tractions at the nodes of the same mesh line for the same loading factor increment.

## 5 CONCLUDING REMARKS

The present study on the conditions for crack opening along mesh lines concurring on a FE “corner node” is carried out in the context of a general research line pursuing the development of new analysis methods for fracture and cracking along mesh lines, which would not require to introduce double-node interfaces along all mesh lines from the beginning of the analysis, but at the same time would verify cracking conditions at “corner nodes” rather than only at “middle nodes” of quadratic elements as in existing literature (Camacho & Ortiz 1996). The study is based on a recent work published by the authors, in which a double minimization method was developed for the calculation of stress tractions along mesh lines concurrent on a corner node, with very few additional assumptions, mainly a crack opening along the mesh lines and the corresponding initial flow rule. The simple example presented illustrates some of the situations which can take place at nodes with four potential crack lines. The results can be however extrapolated easily to nodes with a different number of concurrent mesh lines. Additional details of this study may be found in Ciancio et al. (in press).

## 6 ACKNOWLEDGEMENTS

The first author wishes to thank the support received from MIUR (Italy) and Generalitat de Catalunya (Barcelona) for developing her doctoral thesis. The second author acknowledges research Grants MAT2003-02481 and BIA2006-12717 from MEC (Madrid), and 2005SGR00842 from Generalitat de Catalunya (Barcelona). Research project 2004/33 from MFOM (Madrid) is also gratefully acknowledged.

## REFERENCES

- Caballero, A. & Carol, I. & Lopez, C.M. 2006. 3D Mesos-structural analysis of concrete specimens under uniaxial tension. In *Comput Meth Appl Mech Engng* 195 (52): 7182-7195.
- Camacho, G.T. & Ortiz, M. 1996. Computational modelling of impact damage in brittle materials. In *Int J Solids Struct* 33(20-22):2899-938.
- Carol, I. & Lopez, C.M. & Roa, O. 2001. Micromechanical analysis of quasi-brittle materials using fracture-based interface elements. In *Int J Numer Meth Engng* 52(1/2):193-215.
- Carol, I. & Prat, P.C. & Lopez, C.M. 1997. A normal/shear cracking model. Application to discrete crack analysis. In *ASCE J Engng Mech* 123(8):765-73.
- Ciancio, D. & Carol, I. & Cuomo, M. 2006. On inter-element forces in the FEM-displacement formulation, and implications for stress recovery. In *Int J Numer Meth Engng* 66(3):502-28.
- Ciancio, D. & Carol, I. & Cuomo, M. in press. Crack opening conditions at “corner nodes” in FE analysis with cracking along mesh lines. In *Eng Frac Mech* (2006), doi:10.1016/j.engfracmech.2006.10.005.
- Gens, A. & Carol, I. & Alonso, E. 1988. An interface element formulation for the analysis of soil-reinforcement interaction. *Comput Geotech* 7:133-51.
- Rots, J.G. 1988. Computational Modeling of Concrete. PhD thesis. TU Delft.
- Rots, J.G. & Schellekens J.C.J. 1990. Interface elements in concrete mechanics. In *Bicanic N, Mang H, editors. Computer-aided analysis and design of concrete, Vol. 2. Zell-am-See, Austria: Pineridge Press*; 909-18.
- Sluys, L.J. & Berends, A.H. 1998. 2D/3D modelling of crack propagation with embedded discontinuity elements. In *Computational Modelling of Concrete Structures (EURO-C). Austria: Badgastein* 399-408.